ELSEVIER

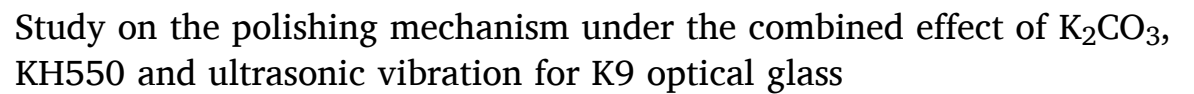
Contents lists available at ScienceDirect

# **Applied Surface Science**

journal homepage: www.elsevier.com/locate/apsusc



## Full Length Article



Sheng Qu<sup>a,b</sup>, Zhijie Cui<sup>c</sup>, Xuchen Chu<sup>c</sup>, Xingwei Sun<sup>a,b</sup>, Zhixu Dong<sup>a,b</sup>, Heran Yang<sup>a,b</sup>, Yin Liu<sup>a,b</sup>, Zixuan Wang<sup>c,\*</sup>, Tianbiao Yu<sup>c,\*</sup>, Ji Zhao<sup>c</sup>

- <sup>a</sup> School of Mechanical Engineering, Shenyang University of Technology, Shenyang 110870, PR China
- b Liaoning Province Key Laboratory of Complex Surface NC Manufacturing Technology, Shenyang 110870, PR China
- <sup>c</sup> School of Mechanical Engineering and Automation, Northeastern University, Shenyang 110819, PR China

#### ARTICLE INFO

Keywords:
K9 optical glass
K<sub>2</sub>CO<sub>3</sub>
KH550
Ultrasonic vibration chemical–mechanical polishing (UV-CMP)

#### ABSTRACT

K9 optical glass plays an important role in the field of optics and optoelectronic information due to its high thermal stability and excellent optical imaging properties. Considering the low polishing efficiency and surface quality from its extremely high hard and brittle properties, a novel SiO<sub>2</sub> polishing slurry containing  $K_2CO_3$  and 3-aminopropyltriethoxysilane ( $C_9H_{23}NO_3Si$ , KH550) is prepared for ultrasonic vibration chemical–mechanical polishing (UV-CMP) of K9 optical glass, and its polishing characteristics and mechanism are investigated. The results demonstrate that  $K_2CO_3$  promotes the material removal rate (MRR) significantly, while the adsorption effect of KH550 reduces the wear ratio and coefficient of friction (COF), and improves the dispersion of SiO<sub>2</sub> abrasive particles and polishing performance of UV-CMP remarkably. Ultrasonic wave further induces softening of surface hydration reaction, homogeneous distribution of abrasive particles and enhances impact and grinding ability of abrasive particles. The optimal MRR is14.5298  $\mu$ m/min and Sa is 54.07 nm at 1.5 wt%  $K_2CO_3$ , 1.6 wt% KH550 and the ultrasonic amplitude of 6  $\mu$ m, indicating that the UV-CMP supplied guidance for multi-field-assisted polishing of hard and brittle materials.

#### 1. Introduction

K9 optical glass, with the main component of SiO<sub>2</sub>, is widely applied as an optical component due to its good reflection, refraction, and transmission in the short visible and infrared wavelengths [1]. Currently, the processing of optical glass undergoes cutting, grinding and polishing [2-4]. Among them, polishing as a crucial step directly affects the imaging accuracy and measurement precision of optical components [5]. There are many conventional polishing methods, such as bonnet polishing (BP), magnetorheological polishing (MRF), laser polishing (LP) and chemical mechanical polishing (CMP) [6–9]. Among them, LP and MRF require extremely high requirements for experimental environments and equipment, which increases the manufacturing cost. BP hinders the manufacture of small optical components due to the material properties and wall thickness of the polishing tool. CMP has a wide range of applications and simple experimental conditions, but the lower processing efficiency does not fully utilize the efficacy of chemical polishing slurries. There is an urgent requirement for a new polishing technique to improve the processing efficiency and surface quality of optical glass, thereby enhancing the performance of optical components. Therefore, a series of multi-energy field-assisted CMP methods have been proposed such as ultraviolet assisted CMP, plasma assisted CMP and ultrasonic vibration CMP (UV-CMP) [10–13]. Among these assisted CMP methods, UV-CMP, as a rapidly developing method, provides a large amount of impact energy for chemical polishing slurries [14,15]. It shows favorable machinability on difficult-to-machine material with hard and brittle characteristics, which can effectively improve surface quality, increase machining efficiency and extend the life of the polishing tool [16].

Many specialists have studied UV-CMP. Tsai et al. [17] utilized CMP and UV-CMP to process copper-based materials, respectively. The experimental results show that the material removal rate (MRR) of UV-CMP is maximally enhanced by 90 % and the surface roughness is reduced to 1.448 nm by 40 % compared with regular CMP. Zhou et al. [18] investigated sapphire UV-CMP. It is found that polishing produces a new softened chemical product Al<sub>2</sub>Si<sub>2</sub>O<sub>7</sub>, which increases the MRR of

E-mail addresses: 2110122@stu.neu.edu.cn (Z. Cui), 2310088@neu.stu.edu.cn (X. Chu), yangheran@sut.edu.cn (H. Yang), wangzx@mail.neu.edu.cn (Z. Wang), tianbiaoyuneu@163.com (T. Yu), zhaojineu@163.com (J. Zhao).

<sup>\*</sup> Corresponding authors.

sapphire UV-CMP by about 60 %, decreases the surface roughness by about 25 %, lowers the surface damage layer thickness by 38 %, and diminishes the residual stresses and the surface crystalline defects. Liu et al.[19] employed ultrasonic elliptical vibration (UEV) technology in combination with chemical mechanical polishing (CMP) for monocrystalline silicon. It is found that the processing efficiency of UEV-CMP reaches about 700 nm/min and the surface roughness decreases to about 11 nm. The softened layer on the single crystal silicon surface can be removed not only by mechanical removal of abrasive particles, but also by ultrasonic vibration action. Chen et al. [20] conducted UV-CMP on SiC. The effects of H<sub>2</sub>O<sub>2</sub> content, FeSO<sub>4</sub> content and ultrasonic amplitude on MRR and surface roughness of UV-CMP are analyzed experimentally and theoretically. The results reveal that the combined action of the ultrasonic wave and the Fenton oxidation reaction achieves upgraded polishing efficiency and surface quality compared with CMP. The maximum MRR obtained is 1350.63  $\mu$ m<sup>2</sup> /min, which is 19.51 % higher than that of CMP, when the polishing slurry with H2O2 concentration of 2.5 wt% and FeSO<sub>4</sub> concentration of 0.025 wt% is applied to UV-CMP on SiC at the ultrasonic amplitude of 6 µm.

In addition, chemical polishing slurry performance has an important influence on the workpiece properties. Polishing slurry additives directly affect the chemical polishing slurry performance. A large number of scholars have explored polishing slurry additives. Liang et al. [21] added sodium citrate (C<sub>6</sub>H<sub>5</sub>Na<sub>3</sub>O<sub>7</sub>) to the polishing slurry for CMP of K9 optical glass. It is found that in the polishing slurry containing 3.0 % CeO<sub>2</sub> abrasive particles, 0.01 % C<sub>6</sub>H<sub>5</sub>Na<sub>3</sub>O<sub>7</sub> improves the abrasive particles' agglomeration and reduces the defects such as pitting and corrosion pits. This decreases the scratches on the polished surface, which in turn reduces the surface roughness of the K9 optical glass. Gold et al. [22] investigated the effect of KCl and KNO3 on the hydration reaction of SiO<sub>2</sub> surfaces at low temperatures. The team shows that the silanol (Si-OH) content is increased significantly in the potassium salt slurry. It is concluded that K<sup>+</sup> is a key factor influencing the CMP of the SiO<sub>2</sub> surface. It reduced the water activity of the slurry and thus increased the Si-OH content of the surface. Xu et al. [23] formulated a polishing slurry containing Na<sub>2</sub>CO<sub>3</sub> and CeO<sub>2</sub> abrasive particles for processing fused silica. The surface roughness of the workpiece reaches 0.093 nm, which is 45 % lower compared with the commercial CeO<sub>2</sub> polishing slurry. Based on the XPS and FTIR results, it is observed that CeO2 forms -Ce-O-Si- structure by chemical reaction during the CMP and surface defects are removed by the mechanical force of the abrasive particles, obtaining a smooth quartz glass surface. Han et al. [24] found that different valence cationic salts (NaCl, CaCl<sub>2</sub>, AlCl<sub>3</sub>) could enhance the material removal rate of silica thin film CMP. However, high valence cations are more vulnerable to particle agglomeration and precipitation under the steady-state conditions of the polishing slurry, due to the stronger effect of high valence cations on the electrostatic interactions between the abrasive particles than that of low valence cations. Xie et al. [25] explored experimentally the effect of NH<sub>4</sub> on the MRR of silicon wafer CMP. When the NH<sub>4</sub><sup>+</sup> concentration was 125 mol/L, the MRR increased to 1687 Å/min, and the polishing slurry maintained good dispersion. COF and XPS measurements showed that NH<sub>4</sub><sup>+</sup> reduced the electrostatic repulsion between silica nanoparticles and silicon wafers while accelerating the chemical reaction between silicon wafers and

Subsequently, surfactants are studied to improve the stability of the chemical polishing slurry and the surface quality of the workpiece. Bu et al. [26] prepared a chemical polishing slurry using sodium dodecyl sulfate (SDS) and performed CMP on shallow trench (STI) structures of  $SiO_2$  material. The results indicated that the surface quality of the polished workpiece is significantly improved, but the MRR is significantly reduced. Li et al. [27] injected a polishing slurry containing cetyl-trimethylammonium bromide ( $C_{16}TAB$ ) into the two  $SiO_2$  interfaces. It is detected that the hydration reaction between C16TAB and two  $SiO_2$  interfaces occurred using the atomic force microscopy (AFM) technique. A double-layer structure is formed to undertake the external force,

which results in the formation of the super lubrication phenomenon. Kim et al. [28] investigated the effect of anionic surfactants on wafers during CMP. Using contact angle experiments, it was found that the polyacrylic acid (PAA) ammonium salts resulted in excellent flowability of  $SiO_2$  abrasive particles and an increase in polishing slurry stability. The MRR of wafers increased significantly with the increase in pH. Penta et al. [29] added sodium dodecyl sulfate, sodium dodecanoyl sarcosine, dodecyl phosphate, and sodium dodecylbenzene sulfonate to the  $SiO_2$  polishing slurry to study the effect of four anionic surfactants on the CMP of silica film, respectively. The experimental results show that the dispersion of  $SiO_2$  abrasive particles increased under an acidic environment, while the material removal rate of  $SiO_2$  films changed less.

From the above analysis, it can be seen that cationic salt plays an important role in MRR enhancement in  $SiO_2$  polishing slurry. The anionic surfactants have little effect on MRR, and cationic surfactants are likely to cause super-lubrication conditions in the polishing. Meanwhile, the two surfactants are susceptible to strong electrolytes, in both acid and alkali environments. Therefore, this study selects a novel surfactant-silane coupling agent 3-aminopropyltriethoxysilane ( $C_9H_{23}NO_3Si$ , KH550). It is an organic silicide containing amino groups and ethoxy groups, which is widely used in the fields of surface modification and material filling [30].

To comprehensively enhance the polishing performance of K9 optical glass, a novel silica polishing slurry containing  $K_2CO_3$  and KH550 was developed. The impact of  $K_2CO_3$  and KH550 on the surface quality and MRR of UV-CMP of K9 optical glass was investigated. The  $K_2CO_3$  and KH550 on the properties and phase transitions of the chemical polishing slurry were investigated for mean particle size, Zeta potential, Polymer dispersity index (PDI), Fourier Transform infrared spectroscopy (FTIR), Coefficient of Friction (COF) and X-ray photoelectron spectroscopy (XPS). Finally, the polishing mechanisms of K9 optical glass in the UV-CMP were systematically investigated in terms of hydration reaction, adsorption mechanism of KH550 and ultrasonic vibration. A novel approach was introduced in this study for the ultrasonic vibration and hydration reaction processing of SiO2 materials, and it has potential applications in K9 optical glass polishing.

### 2. Material and methods

In this paper, colloidal silica (Jinghuo Technology Glass Co., Ltd., Dezhou, China) with an average size of 0.05  $\mu m$ , was chosen as a polishing abrasive particle,  $K_2CO_3$  (Sinopharm Chemical Reagent Co., Ltd, China) as a cationic salt additive. The silane coupling agent KH550 (Sinopharm Group Chemical Reagent Co. Ltd, China) was used as a novel surfactant. It contains amino groups and silane oxides. Deionized water was utilized as a solvent for the preparation of the polishing slurry.

Steps in the preparation of chemical polishing slurry: First, colloidal silica was dissolved in deionized water to adjust the  $SiO_2$  abrasive particles to 12 wt%. Then  $K_2CO_3$  was weighed using a precision balance and dispersed by ultrasonication to fully dissolve it at  $25\,^{\circ}C$  for 30 min. According to the previous experimental results, the pH value of the polishing slurry is between  $11.5\,$  and  $12\,$ , which ensures the stability of the  $SiO_2$  abrasive particles and enhances the chemical action of the polishing slurry to achieve a high MRR [31]. Finally, KH550 was gradually dripped into the slurry and the pH of the slurry was adjusted to  $12\,$ . The slurry was stirred in a magnetic mixer to fully hydrolyze the KH550 and mixed at  $70\,^{\circ}C$ ,  $300\,$  rpm, and  $60\,$  min. The hydrolysis reaction of KH550 is shown in Fig.  $1.\,$ 

The workpieces for UV-CMP experiments were split into 50 mm  $\times$  50 mm  $\times$  4 mm K9 optical glass. The SiO<sub>2</sub> is the main component and provides the basic structure and hardness of the K9 optical glass. It also contains oxides such as B<sub>2</sub>O<sub>3</sub>, BaO and As<sub>2</sub>O<sub>3</sub>, which contribute to the optical properties of the glass[32]. The workpieces were cleaned in an ultrasonic cleaner containing anhydrous ethanol for 20 min before and after experiments to remove surface impurities and subsequently dried

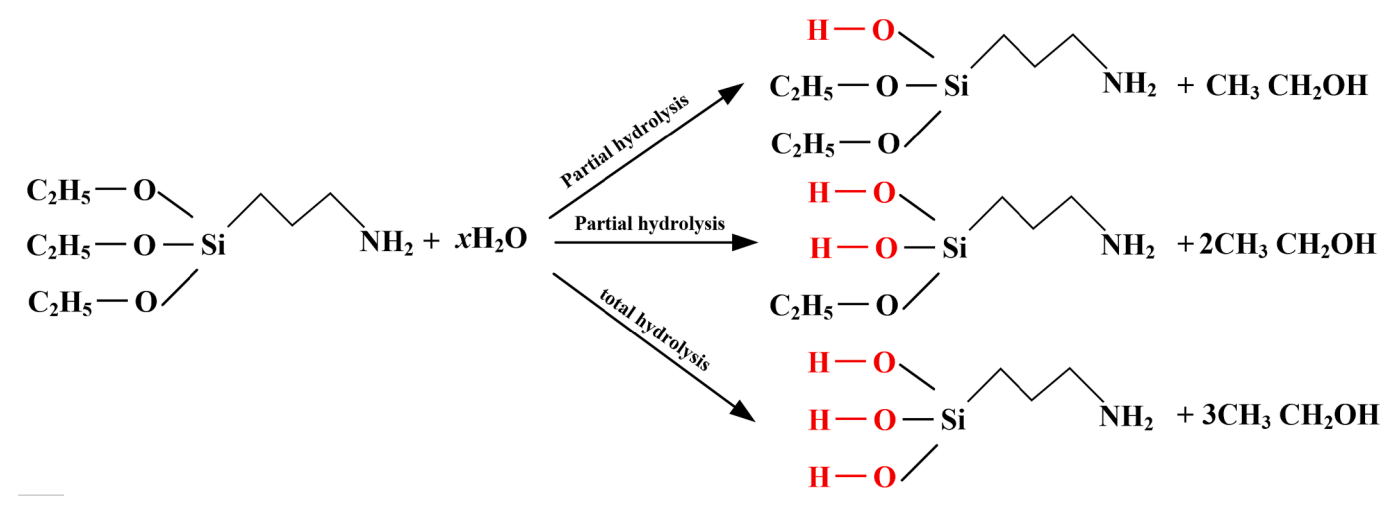


Fig. 1. Schematic diagram of KH550 hydrolysis reaction.

in a drying oven. The polishing pad was selected from a porous polyurethane material with a 12 mm diameter cylindrical polishing tool. The experiments were conducted on a self-constructed ultrasonic vibration polishing machine tool with 300 mm X/Y/Z axis guide rail travel, as shown in Fig. 2. The frequency of the ultrasonic spindle is 25 kHz, the ultrasonic amplitude is 0–10  $\mu m$ , and the speed range is 0–24,000 rpm. The frequency of ultrasonic atomization is 55 kHz and the flow rate of the peristaltic pump is 0.1–0.5 ml/s. The polishing force is adjusted utilizing a cylinder and a pressure sensor. UV-CMP experiments are performed on K9 optical glass using the prepared SiO2 chemical polishing slurry. The flow rate of ultrasonic atomization is 0.2 ml/s, the

rotational speed of the polishing tool is 3000 rpm, the ultrasonic amplitude is 3  $\mu$ m, the feed rate is 0.015 mm/s, and the polishing time is 30 min.

The mean size, PDI and zeta potential of the abrasive particles, which are important criteria for evaluating the performance of the chemical polishing slurry, were measured using a nanoparticle size and zeta potential analyzer (Anton Paar, litesizer 500) and a laser particle sizer (Malvern, Mastersizer 3000), respectively.

To explore the effect of additives on the tribological properties during the polishing process, friction and wear experiments were carried out on a reciprocating friction and wear tester (MFT-4000) with

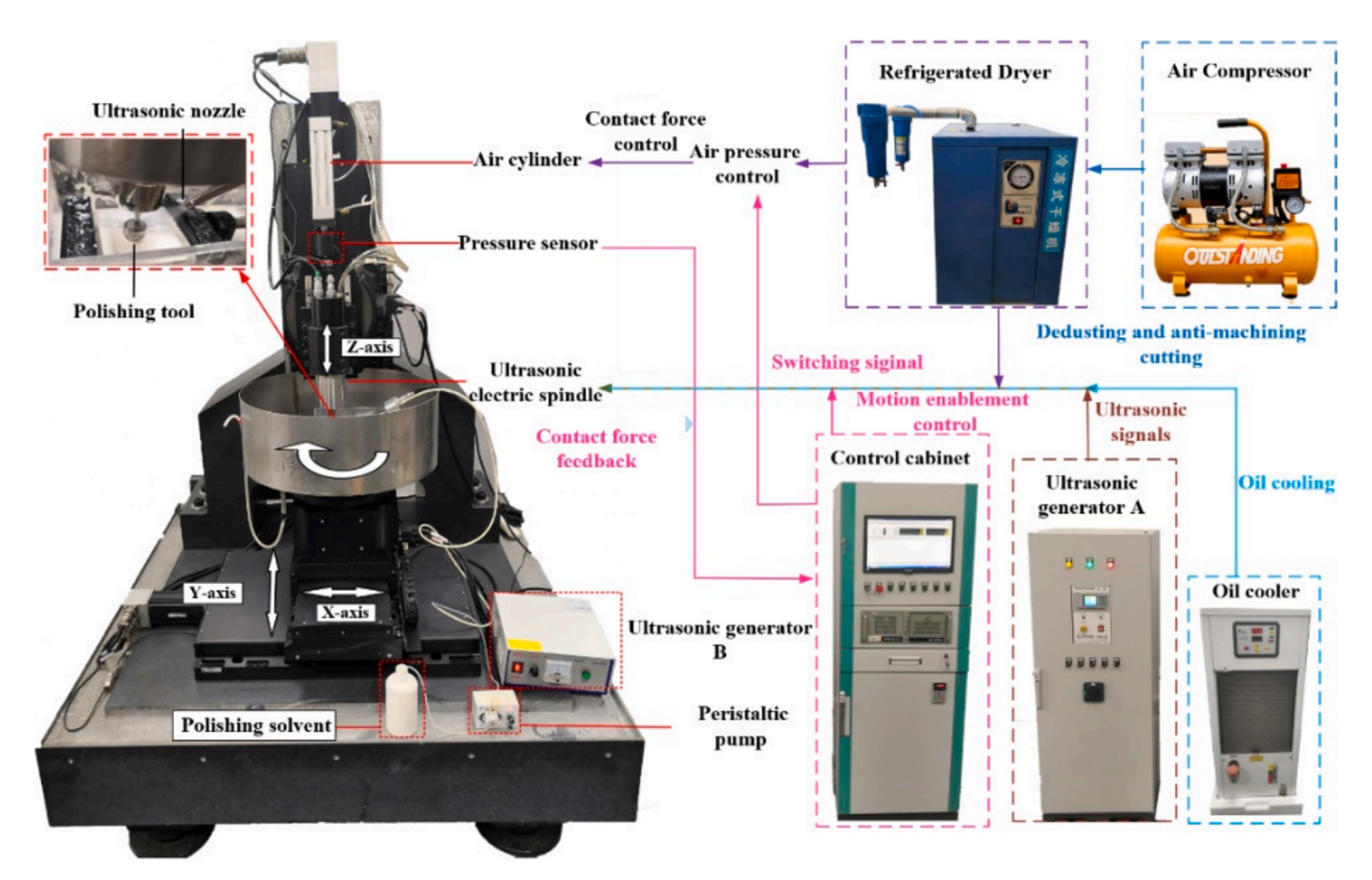


Fig. 2. Ultrasonic vibration polishing machine tool.

different  $K_2CO_3$  and KH550 concentrations. The experiments were carried out on the K9 optical glass surface with reciprocal scraping for 20 min, friction speed of 200 mm/min, pressure load of 10 N, abrasive ball of  $Al_2O_3$ , and wear distance of 4 m. The fixed component during the experiment was 10 wt%  $SiO_2$  abrasive particles, pH = 12, and the variable components were  $K_2CO_3$  and KH550 concentration. The tribological properties of the additives were investigated using COF versus time, mean COF and wear ratio.

To investigate the effect of  $K_2CO_3$  on the hydration reaction on the K9 optical glass surface as well as the adsorption properties of KH550 on the K9 optical glass surface in an alkaline solution, the surface elemental valence changes were analyzed by XPS using X-ray photoelectron spectroscopy (Thermo Scientific, K-Alpha). Firstly, the K9 optical glass was immersed for 360 min in different component solutions respectively, as shown in Table 1. Then it was removed, rinsed with deionized water and blown dry with compressed air. Finally, the XPS spectra were analyzed by peak splitting and fitting with Thermo Avantage software. Before analyzing the data, it is necessary to calibrate the energy spectrum based on the C1s with the binding energy of 284.8 eV and to determine the chemical bonding of the elements on the K9 optical glass surface through the curve changes and energy shifts [33,341].

To characterize the changes in chemical bonding and molecular vibration before and after the modification of  $\mathrm{SiO}_2$  abrasive particles by KH550, this paper was carried out by FTIR analysis using a Fourier transform infrared spectrometer (Thermo Scientific Nicolet iS50). Firstly, the KH550 was stirred at 70 °C for 180 min using a magnetic mixer to fully hydrolyze it and slowly added into the diluted colloidal silica slurry to mix thoroughly. Next, the slurry was completely centrifuged and the precipitate was filtered and dried to obtain the KH550-modified  $\mathrm{SiO}_2$  abrasive particles. Finally, it was mixed with KBr and dried in an oven, and samples were prepared in a tablet press for an infrared spectrometer.

The surface roughness Sa, MRR were measured by laser scanning confocal microscope (LSCM, OLS4100) from Olympus. To reduce random errors, the workpiece was measured at three random locations and the mean value was taken as the surface roughness of the workpiece. In addition, the entire workpiece surface before and after polishing, friction and wear experiments was also laser scanned with the aid of the LSCM, and the maximum material removal depth  $D_{remove}$  between the removal profile and the initial flat surface was measured by the equipment's software to calculate the MRR or wear ratio during the polishing time t.

$$MRR = \frac{D_{remove}}{t} \tag{1}$$

#### 3. Results and discussion

#### 3.1. Effect of $K_2CO_3$ on the polishing slurry performance

The dispersion of abrasive particles in the polishing slurry is related to the concentration of the ionic salt additive and is characterized utilizing the PDI value and the mean particle size. The smaller the PDI value, the better the dispersion of the abrasive particles and the more uniform the abrasive particle size. Fig. 3 illustrates the effect of  $K_2CO_3$  concentration on abrasive particle size and PDI value. When no ionic salt additive is added, the  $SiO_2$  abrasive particles are dispersed properly in the polishing slurry, with the mean particle size of 50.5 nm, and the

**Table 1**Solution compositions for workpiece immersion before XPS inspection.

No.	Components
1	deionized water
2	deionized water, $PH = 12$
3	deionized water, $K_2CO_3$ (1.5 wt%), PH = 12
4	deionized water, $K_2CO_3$ (1.5 wt%), KH550 (1.6 wt%), PH = 12

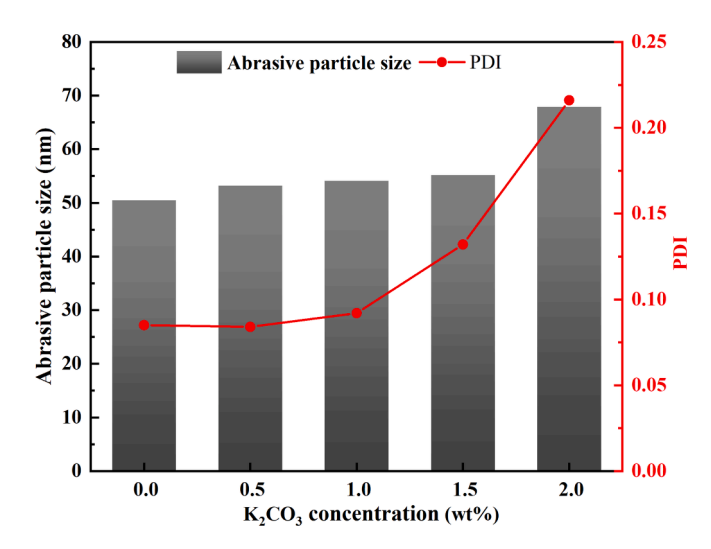


Fig. 3. Effect of K<sub>2</sub>CO<sub>3</sub> concentration on abrasive particle size and PDI.

distribution of abrasive particle size between 50 nm and 70 nm. When the  $\rm K_2CO_3$  concentration is lower than 1.5 wt%, the mean size of the abrasive particles increased slightly compared with that without addition. As the concentration is increased to 2 wt%, the mean abrasive particle size is significantly increased to 67.9 nm, which is a 34.46 % increase compared with no addition. The experimental results are consistent with the findings of Wonseop Choi et al [35].

The effect of  $K_2CO_3$  concentration on the PDI value follows the same trend as that on the mean size of the abrasive particles. The PDI value increased gradually with the  $K_2CO_3$  concentration with the  $K_2CO_3$  concentration lower than 1.5 wt%. However, when the  $K_2CO_3$  concentration reached 2 wt%, the PDI value increased to 0.216.

A large number of hydroxyl groups (OH $^-$ ) are absorbed on the SiO<sub>2</sub> abrasive particle. The hydroxyl groups on the colloidal silica surface hydrolyze with OH $^-$  to form SiO $^-$ , which subsequently reacts with K $^+$  to form Si-OK, the chemical reaction is shown as follows [36]:

$$\equiv Si - O - Si \equiv +OH^- + K^+ \rightarrow SiOK + H_2O \tag{2}$$

In addition, the Si-OK size is larger than the Si-OH size, causing an increase in the  $SiO_2$  abrasive particle size. In the alkaline slurry, cations adsorb on the  $SiO_2$  abrasive particle surface and attract negative charges, so that the adsorption layer with the negative charge and the diffusion layer with the positive charge on the abrasive particle surface form a double electric layer structure [37].

According to the Derjaguin-Landau-Verwey-Overbeek (DLVO) theory, it is known that there are attractive forces and repulsive forces between  $\mathrm{SiO}_2$  abrasive particles, which makes van der Waals potential energy and electrostatic potential energy exist[38,39]. The two potential energies are relevant to the distance between the abrasive particles and also determine the stability of the chemical polishing slurry[40]. The interaction potential energy ( $U_{total}$ ) between the abrasive particles is the sum of the van der Waals potential energy ( $U_{wa}$ ) and the electrostatic potential energy ( $U_{er}$ ) as shown below:

$$U_{total} = U_{wa} + U_{er} \tag{3}$$

The van der Waals potential energy between the abrasive particles in the chemical polishing slurry is expressed as:

$$U_{wa} = -\frac{A_{Ha}R_{abr}}{6H_{2R_{abr}}} \tag{4}$$

The electrostatic potential energy between the abrasive particles in the chemical polishing slurry is expressed as:

$$U_{er} = \pi \varepsilon_o \varepsilon_w R_{\rm abr} \left( 2\xi_1 \xi_2 \ln(\frac{1+e^{-k_{\rm debye}H_{\rm 2R_{abr}}}}{1-e^{-k_{\rm debye}H_{\rm 2R_{abr}}}}) + (\xi_1^2 + \xi_2^2) \ln(1-e^{-k_{\rm debye}H_{\rm 2R_{abr}}}) \right)$$

where  $A_{Ha}$  is the Hamaker constant in the vacuum state of the abrasive particle;  $H_{2Rabr}$  is the distance between two abrasive particles;  $\varepsilon_0$  is the dielectric constant in the vacuum state, which is  $8.854 \times 10^{-12}$  CV $^{-1}$ m $^{-1}$ at 25°C;  $\varepsilon_w$  is the relative dielectric constant in water;  $\xi_1$  and  $\xi_2$  are the zeta potential values of the abrasive particle surface, respectively.  $k_{debye}$  is the debye length, which is associated with the concentration and valence of the electrolyte.

The variation of the interaction potential energy  $U_{total}$  between the abrasive particles is shown in Fig. 4. As the SiO<sub>2</sub> abrasive particles approach each other, the van der Waals potential energy  $U_{wa}$  decreases while the electrostatic potential energy  $U_{er}$  increases. This shift results in a distinctive peak on the interaction potential energy curve, termed the energy barrier. The energy barrier prevents the SiO<sub>2</sub> abrasive particles from contacting each other, so that the SiO<sub>2</sub> abrasive particles need to overcome the energy barrier to contact. As the energy barrier decreases, the SiO<sub>2</sub> abrasive particles are more likely to contact each other more readily, which completely destabilizes the polishing slurry and leads to agglomeration of the SiO<sub>2</sub> abrasive particles. The change in electrolyte concentration of the polishing slurry drives the change in the energy barrier. The stability of the polishing slurry depends on the balance between the van der Waals potential energy  $U_{wa}$  and the electrostatic potential energy  $U_{er}$ .

At low  $K_2CO_3$  concentration, it will cause the van der Waals potential energy  $U_{wa}$  to decrease. The electrostatic potential energy  $U_{er}$  is larger than the van der Waals potential energy  $U_{wa}$ , the adhesion state between  $SiO_2$  abrasive particles is reduced due to Brownian motion, and the interaction potential energy  $U_{total} > 0$ , so that the silicon slurry maintains a stable state. As the  $K_2CO_3$  concentration continues to increase, the van der Waals potential energy  $U_{wa}$  is virtually unaffected, but the bilayer thickness on the  $SiO_2$  abrasive particle surface is compressed, resulting in a decrease in the electrostatic potential energy  $U_{er}$  and a decrease in the energy barrier value. When the abrasive particles overcome the energy barrier and the van der Waals potential energy  $U_{wa}$  is greater than the electrostatic potential energy  $U_{er}$ , the interaction potential energy  $U_{total} < 0$ . As a result, the stability of the colloidal silica decreases, and the abrasive particles tend to settle, resulting in the instability of the colloidal silica system [41,42].

Fig. 5 shows the effect of  $K_2\mathrm{CO}_3$  concentration on the zeta potential of the chemical polishing slurry. When the absolute value of zeta potential is greater than 30 mV (red straight line), the chemical polishing slurry lies in a stable condition. On the contrary, when its value is less

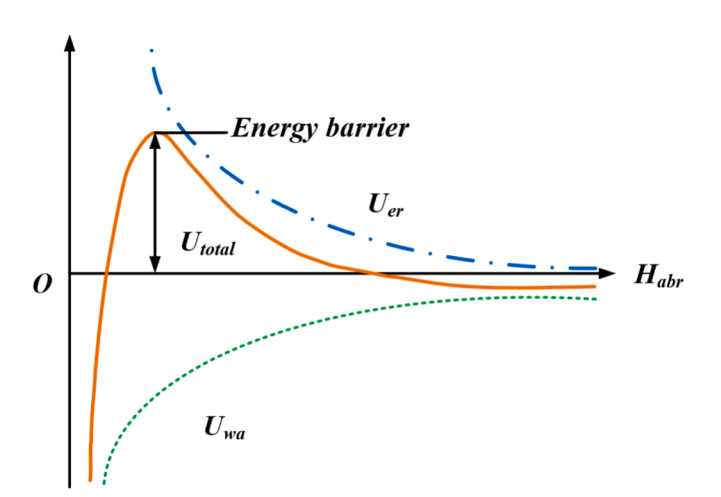


Fig. 4. Interaction potential energy  $U_{total}$  versus distance between abrasive particles.

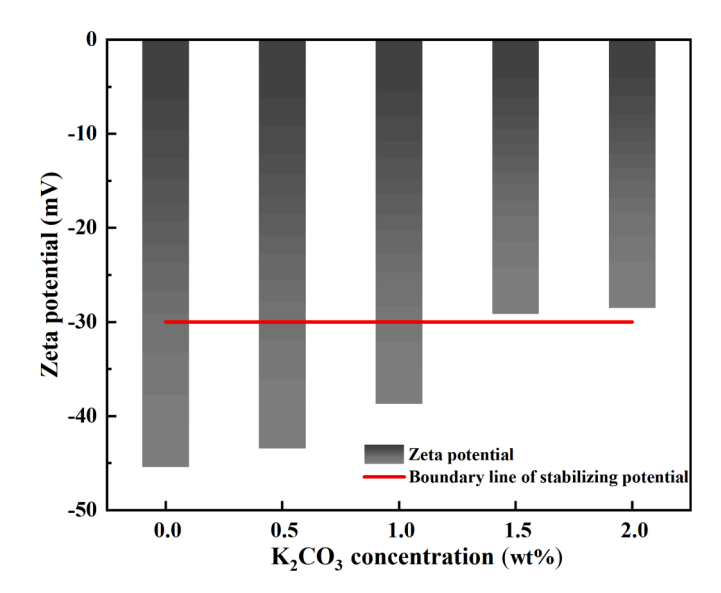


Fig. 5. Effect of K<sub>2</sub>CO<sub>3</sub> concentration on zeta potential.

than 30 mV, the chemical polishing slurry lies in a nonstable state [43,44]. As shown in Fig. 5, the zeta potential increases from  $-45.43\,\text{mV}$  to  $-38.72\,\text{mV}$  as the  $K_2\text{CO}_3$  concentration increases from 0 to 1 wt%. However, when the concentration reaches 1.5 wt%, the zeta potential is  $-29.16\,\text{mV}$ . In the low  $K_2\text{CO}_3$  concentration, the electrostatic repulsion ensures the dispersion of  $SiO_2$  abrasive particles, and the chemical polishing slurry remains in a stable state. However, excessive amounts of  $K_2\text{CO}_3$  significantly increase the aggregation of the abrasive particles so that the chemical polishing slurry becomes unstable.

#### 3.2. Effect of $K_2CO_3$ on polishing performance

The effect of  $K_2CO_3$  on MRR can be observed in Fig. 6. When the concentration of  $K_2CO_3$  is from 0.5 wt% to 2 wt%, the MRR increases continuously with the increase of  $K_2CO_3$ , and the MRR improves from 10.1342  $\mu$ m/min to 13.1785  $\mu$ m/min, which is an increase of 30.04 %. However, the MRR decreases slightly at the 2.5 wt%  $K_2CO_3$ . It is analyzed that the addition of  $K_2CO_3$  promotes the hydration reaction rate on the K9 optical glass surface, which results in rapid material removal from the optical glass surface in the presence of SiO<sub>2</sub> abrasive particles [36]. As a result, the MRR is increased. When  $K_2CO_3$  continued

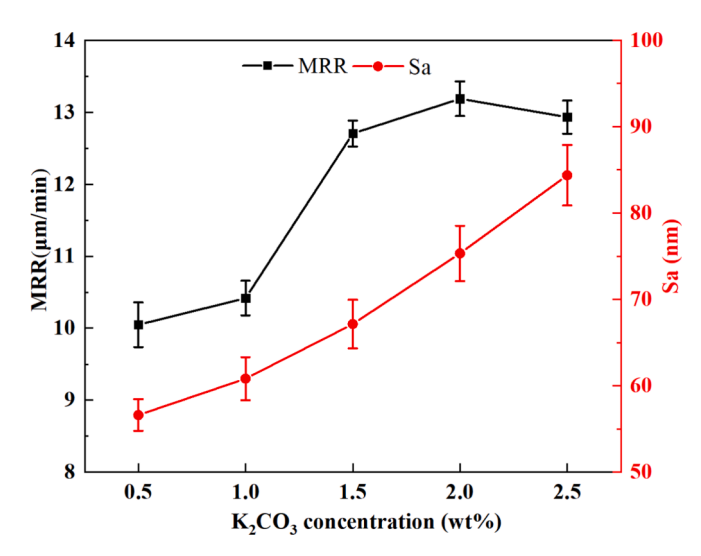


Fig. 6. Effect of  $K_2CO_3$  concentration on the polishing results of K9 optical glass.

to increase, the excess  $K^+$  led to agglomeration of  $SiO_2$  abrasive particles, which resulted in the attraction potential energy greater than the repulsion potential energy of  $SiO_2$  abrasive particles [37]. The agglomeration of  $SiO_2$  abrasive particles leads to a reduction of effective abrasive particles, resulting in a slight decrease in MRR.

As shown in Figs. 6 and 7, with the increase of  $K_2CO_3$ , the Sa of K9 optical glass gradually increases and the surface quality decreases significantly from 56.61 nm at 0.5 wt%  $K_2CO_3$  to 84.37 nm at 2.5 wt%  $K_2CO_3$ , with the Sa value increasing by 49.04 %. This is mainly because the negative charge of the  $SiO_2$  abrasive particle surface is neutralized by  $K^+$ , leading to a decrease in the dispersion of  $SiO_2$  abrasive particles. During UV-CMP of K9 optical glass, the  $SiO_2$  abrasive particles impact the workpiece surface, which leads to non-uniformity in the size and distribution of pits on the microscopic surface. As a result, the Sa value increases and the surface quality decreases.

### 3.3. Effect of $K_2CO_3$ on tribological properties

Fig. 8(a) illustrates the COF curves with  $K_2CO_3$  concentration and wear time for K9 optical glass under a pressure load of 10 N. The COF curves oscillate more in the initial stage, when the shear stress is much larger than the fracture strength of K9 optical glass, leading to the dense crack generation. Subsequently, the cracks expand staggeringly and produce brittle flakes under the effect of the reciprocating shear stress, and gradually reach a steady state, and the COF tends to stabilize. Therefore, the curves for the last 5 min were selected for calculating the

mean COF.

The wear removal volume per unit load and per unit length is known as the wear ratio. It can be seen from Fig. 8(b) that in the absence of  $K_2CO_3,$  the COF is 0.351 and the wear ratio is 1.876  $\times~10^{-4}~mm^3~N^{-1}$ m<sup>-1</sup>. When the K<sub>2</sub>CO<sub>3</sub> concentration increased from 0.5 wt% to 2 wt%, the mean COF increased from 0.358 to 0.393 and the wear ratio increased from 2.013  $\times$   $10^{-4}$  mm  $^3$   $N^{-1}$  m  $^{-1}$  to 3.134  $\times$   $10^{-4}$  mm  $^3$   $N^{-1}$ m<sup>-1</sup>. The mean COF and wear ratio were higher than those without addition. This is mainly attributed to the fact that K2CO3 promotes the hydration reaction between the chemical polishing slurry and the K9 optical glass surface, and forms a hydration layer. The hydration layer is lower in hardness compared with the grinding ball, which tends to insert deeper into the K9 optical glass surface and increase the sliding resistance, resulting in a slight increase in the mean COF. The hydration reaction rate rises with the increase of K2CO3 concentration, and the hydrated layer can be removed rapidly by the grinding ball, which causes a significant increase in the wear ratio.

#### 3.4. Effect of $K_2CO_3$ on the hydration reaction of K9 optical glass

The Si2p spectra shown in Fig. 9 contain two peaks which can be considered as the characteristic peak of  $SiO_2$  located at 103 eV and the characteristic peak of Si-OH at 102.5 eV according to Srikar Rao et al [45]. In Table 1, the peak area ratios of  $SiO_2$  and Si-OH for sample 1 immersed in deionized water are 86.51 % and 13.49 %, respectively. When sample 2 is immersed in deionized water at pH = 12, the peak area

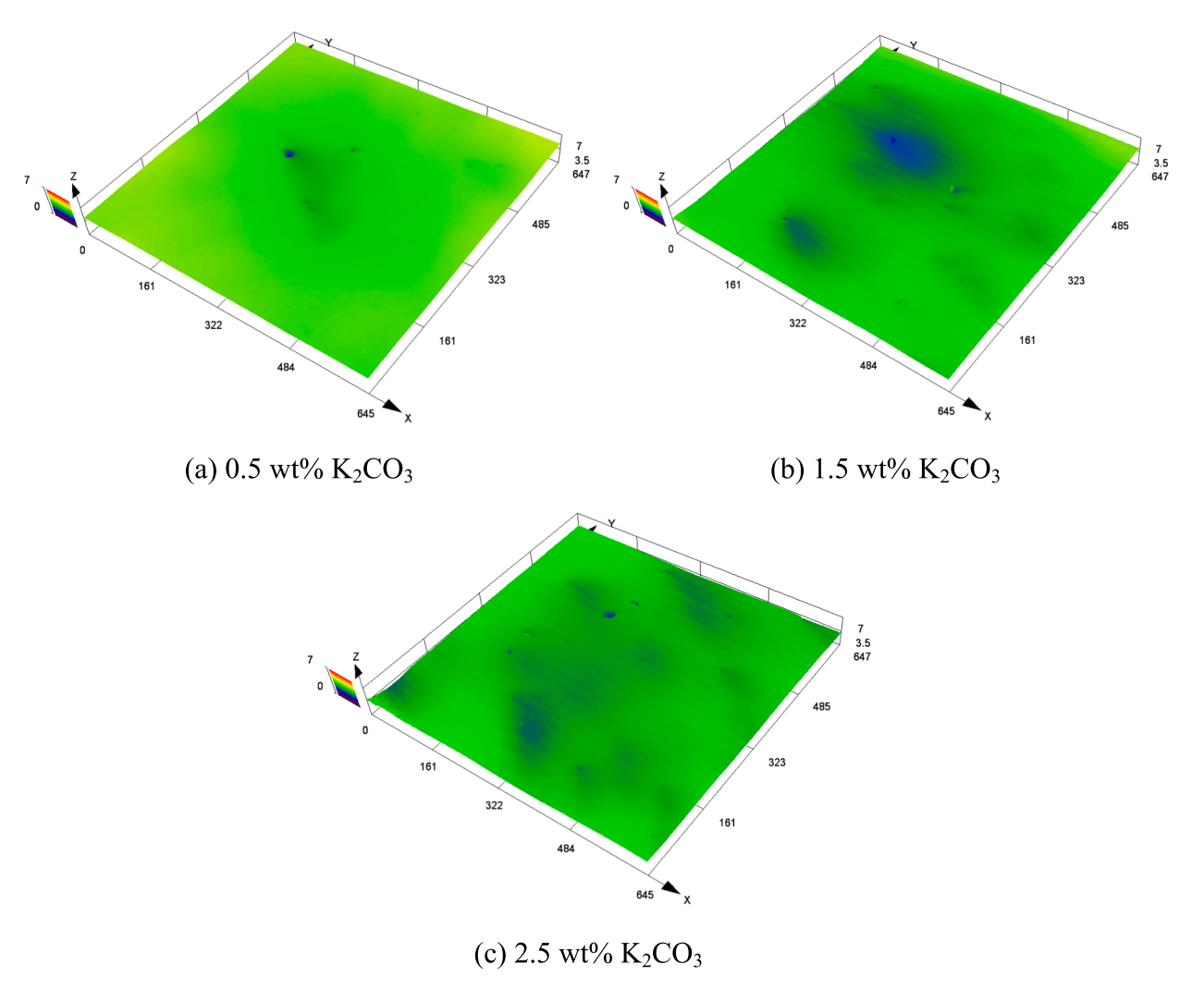
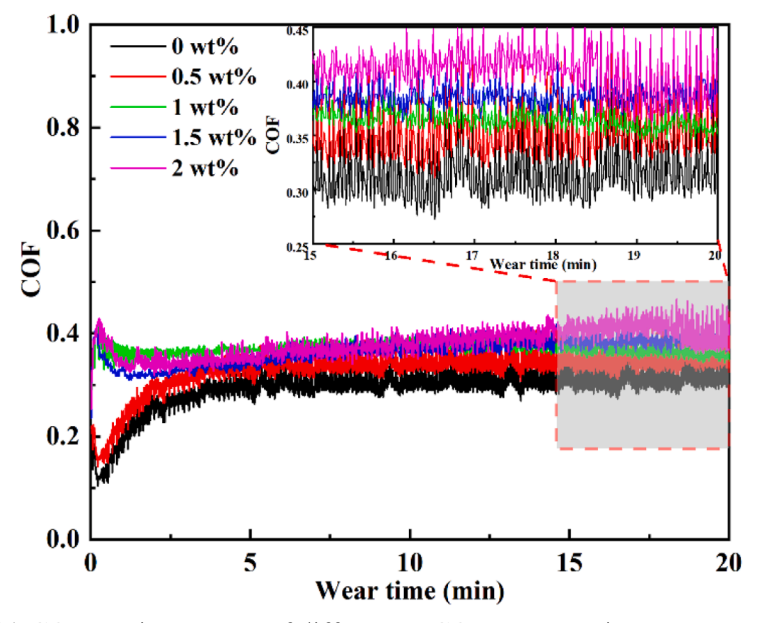
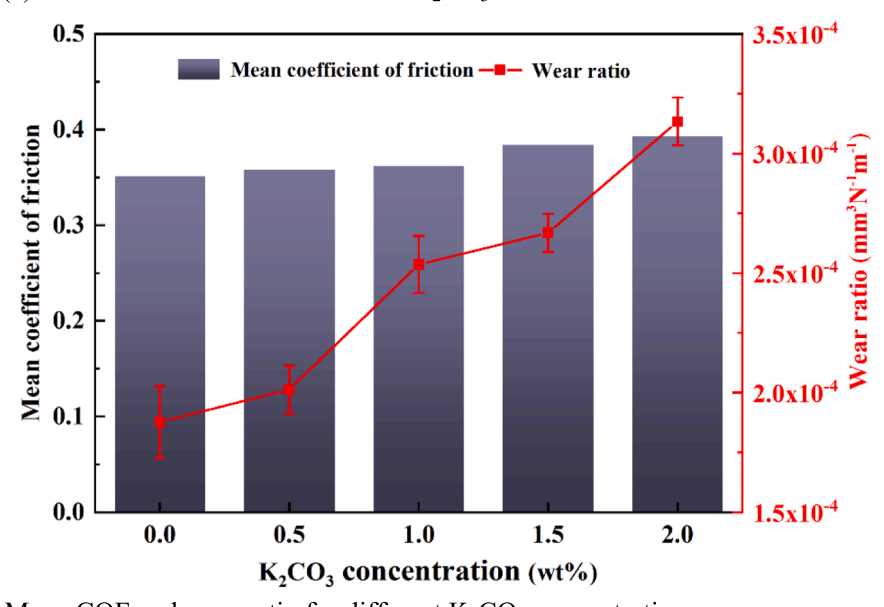


Fig. 7. Surface microstructure of K9 optical glass polished with different K2CO3 concentration.



(a) COF vs. time curves of different K<sub>2</sub>CO<sub>3</sub> concentrations



(b) Mean COF and wear ratio for different K<sub>2</sub>CO<sub>3</sub> concentrations

Fig. 8. Effect of K<sub>2</sub>CO<sub>3</sub> concentrations on COF and wear ratio.

ratio of  $\rm SiO_2$  decreases to 81.85 %, and the peak area ratio of Si-OH increases to 18.15 %.

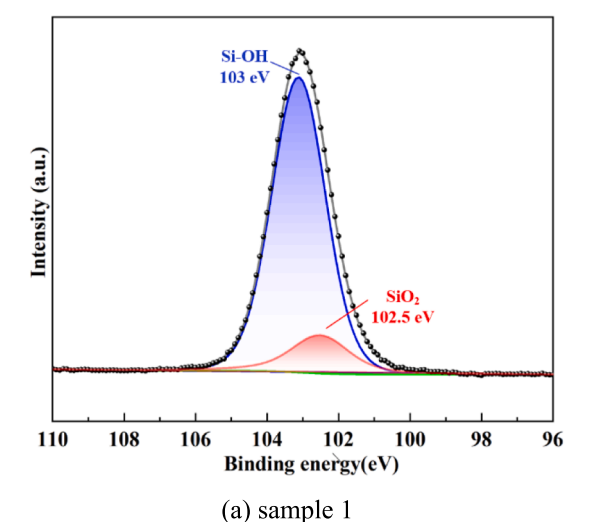
Sample 3 is immersed in deionized water with 1.5 wt%  $K_2CO_3$  and pH=12, the peak area ratio of  $SiO_2$  further decreases to 79.94 %, and the peak area ratio of Si-OH further increases to 20.06 %. From the above XPS spectral analysis, the peak area ratio of  $SiO_2$  decreases and the peak area ratio of Si-OH increases with the introduction of alkaline solution and  $K_2CO_3$ . The hydration reaction is weak under the deionized water. However, the alkaline condition and  $K_2CO_3$  can further intensify the hydration reaction, promoting the breakage of Si-O-Si bond and the generation of Si-OH bond on the K9 optical glass surface. The optical glass has a dense Si-O-Si three-dimensional spatial structure, which is softened into a loose porous structure after the hydration reaction, thus enhancing the thickness of the surface hydration layer [46,47].

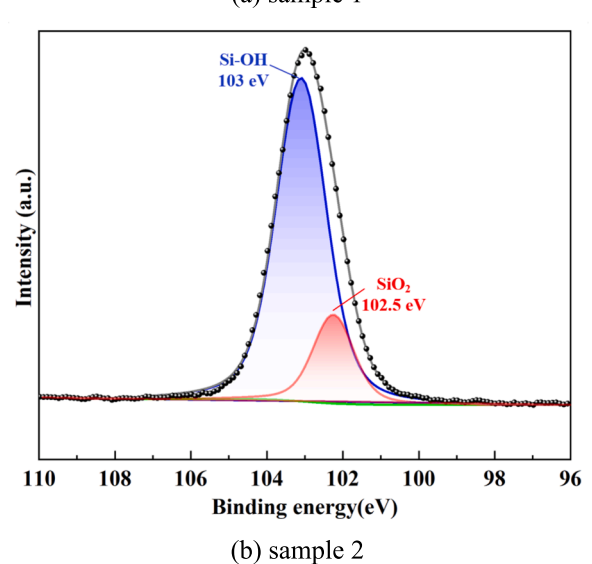
In summary, the introduction of  $K^+$  in the alkaline solution decreases the electrostatic repulsion between the abrasive particles and the optical glass surface, which improves the mechanical removal of the abrasive

particles in the UV-CMP, accelerates the hydration reaction rate and increases the surface hydration layer thickness. The XPS Si2p measurements shown in Fig. 8 can well explain the MRR changes of UV-CMP.

#### 3.5. Effect of KH550 on the polishing slurry performance

Fig. 10(a) shows the effect of KH550 concentration on  $SiO_2$  abrasive particle size and PDI. The mean size of the  $SiO_2$  abrasive particle is 55.19 nm when only 1.5 wt%  $K_2CO_3$  is added. The mean size of  $SiO_2$  abrasive particle increases from 55.47 nm to 58.61 nm with the increase of KH550 concentration from 0 wt% to 1.6 wt%, with a maximum increase of 6.20 %. This is mainly attributed to the hydrolyzed polymer of KH550 adsorbed on the  $SiO_2$  abrasive particle surface. The PDI value decreases sharply with the increase of KH550 concentration from 0.132 at 0 wt% to 0.054 at 1.6 wt%. The distribution of abrasive particles tends to be homogeneous, and dispersibility gradually becomes better. This





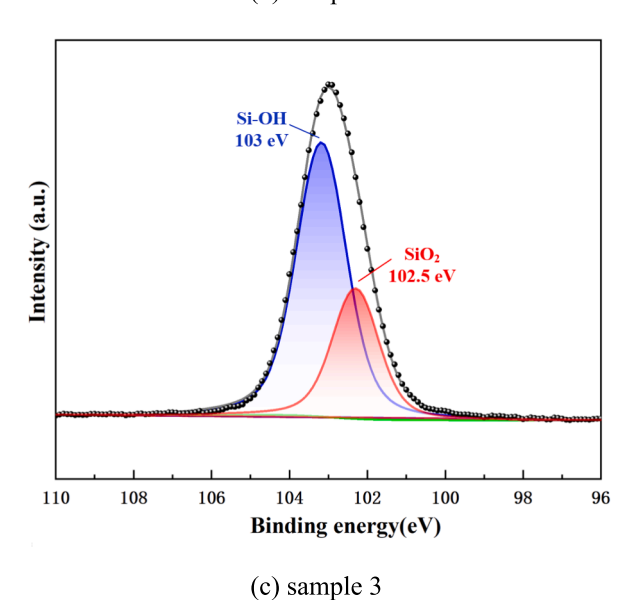
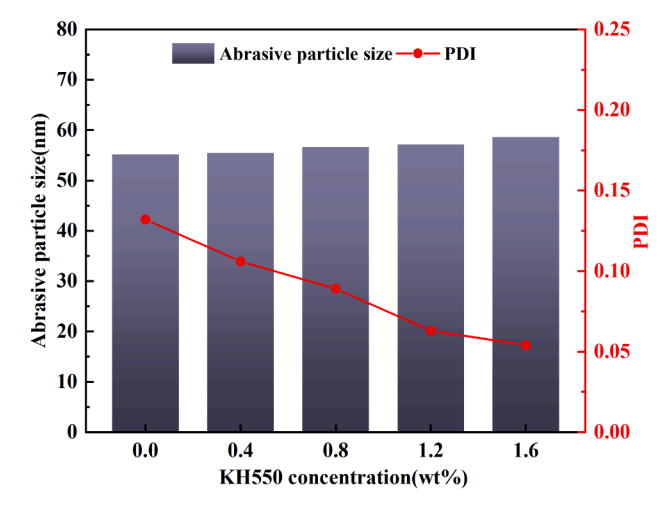
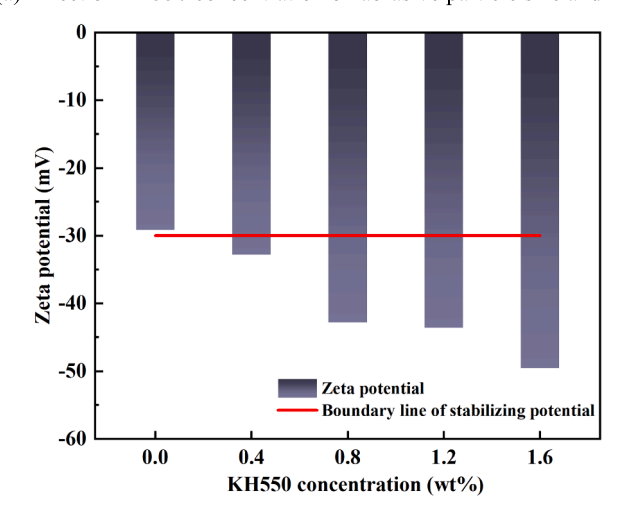


Fig. 9. Si2p spectra of optical glass surface.



(a) Effect of KH550 concentration on abrasive particle size and PDI



(b) Effect of KH550 concentration on zeta potential

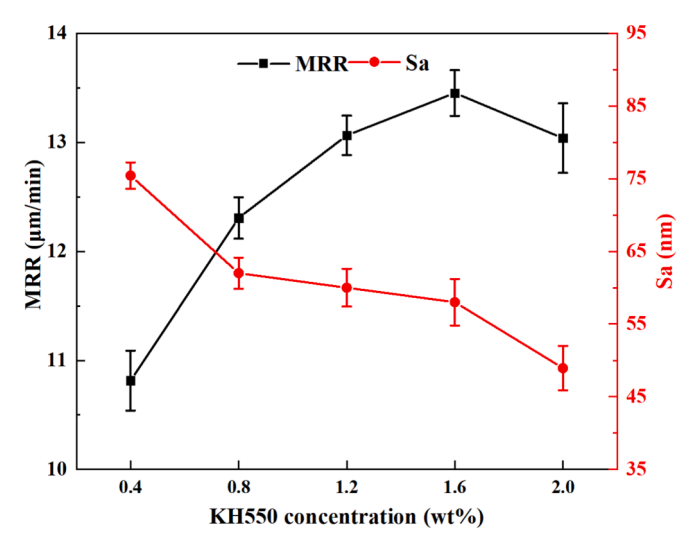
Fig. 10. Effect of KH550 concentration on the polishing slurry performance.

indicates that the addition of KH550 can improve the dispersion of  $\rm SiO_2$  abrasive particles in the chemical polishing slurry. Fig. 10(b) shows the effect of KH550 on the zeta potential of the chemical polishing slurry. The absolute value of zeta potential increased with increasing KH550. The zeta potential decreases from -29.16 mV to -49.55 mV when the KH550 is increased from 0 wt% to 1.6 wt%, an increase of 69.92 % in absolute value.

The experimental results are explained as: Due to the amino group hydrolyzed by KH550 and grafted to the  $\mathrm{SiO}_2$  abrasive particle surface, which caused the grafted side chains to extend outward and increased the steric hindrance effect between the abrasive particles. The longer the side chain, the more obvious the spatial resistance effect [48]. The zeta potential of the chemical polishing slurry decreases, the repulsion force between  $\mathrm{SiO}_2$  abrasive particles increases, and the dispersion of the chemical polishing slurry increases.

#### 3.6. Effect of KH550 on polishing performance

The effect of KH550 on the MRR of K9 optical glass can be observed in Fig. 11. The MRR increases gradually when KH550 concentration is between 0.4 wt% and 1.6 wt%. It increased from 10.8141  $\mu m/min$  to 13.4518  $\mu m/min$ , an increase of 24.39 %. However, when the KH550 concentration was increased to 2.0 wt%, the MRR decreased slightly to 13.0382  $\mu m/min$ . This phenomenon can be attributed to the fact that the increase in KH550 concentration enhances the repulsive force between



 ${f Fig.~11.}$  Effect of KH550 concentration on the polishing results of K9 optical glass.

the  $SiO_2$  abrasive particles, which improves the dispersion and the mechanical removal ability of  $SiO_2$  abrasive particles, leading to an increase in MRR. However, excessive KH550 significantly reduces the

friction between  $SiO_2$  abrasive particles and the polished contact area due to the adsorption of KH550, resulting in a decrease in MRR.

The effect of KH550 concentration on the surface morphology and surface roughness Sa of K9 optical glass are shown in Figs. 11 and 12. The Sa decreases gradually with the increase of KH550 concentration. It decreases from 75.42 nm at 0.4 wt% to 48.93 nm at 2 wt%, a decrease of 35.12 %. It is analyzed that the abrasive particles are dispersed homogeneously with the increase of KH550 concentration. In addition, due to the strong adsorption of KH550 itself, it covers the craters on the workpiece surface, which reduces the chemical reaction rate at the craters and decreases the mechanical removal probability of SiO2 abrasive particles on the workpiece surface. Instead, the surface bumps are more likely to be removed by abrasive particles, which leads to improved surface quality.

#### 3.7. Effect of KH550 on tribological properties

Fig. 13(a) shows the COF curve with KH550 concentration and wear time. The COF curves for KH550 show less fluctuation compared with those for  $K_2 CO_3$ . Again, the curves for the last 5 min were chosen to calculate the mean COF. As can be seen in Fig. 13(b), the mean COF is 0.384 and the wear rate is  $2.6680\times 10^{-4}\, \text{mm}^3\, \text{N}^{-1}\, \text{m}^{-1}$  without KH550. When the KH550 concentration is increased from 0.4 wt% to 1.6 wt%, the mean COF decreases from 0.363 to 0.311, and the wear ratio gradually decreases from 2.4945  $\times$   $10^{-4}\, \text{mm}^3\, \text{N}^{-1}\, \text{m}^{-1}$  to 2.1930  $\times$   $10^{-4}\, \text{cm}^3$ 

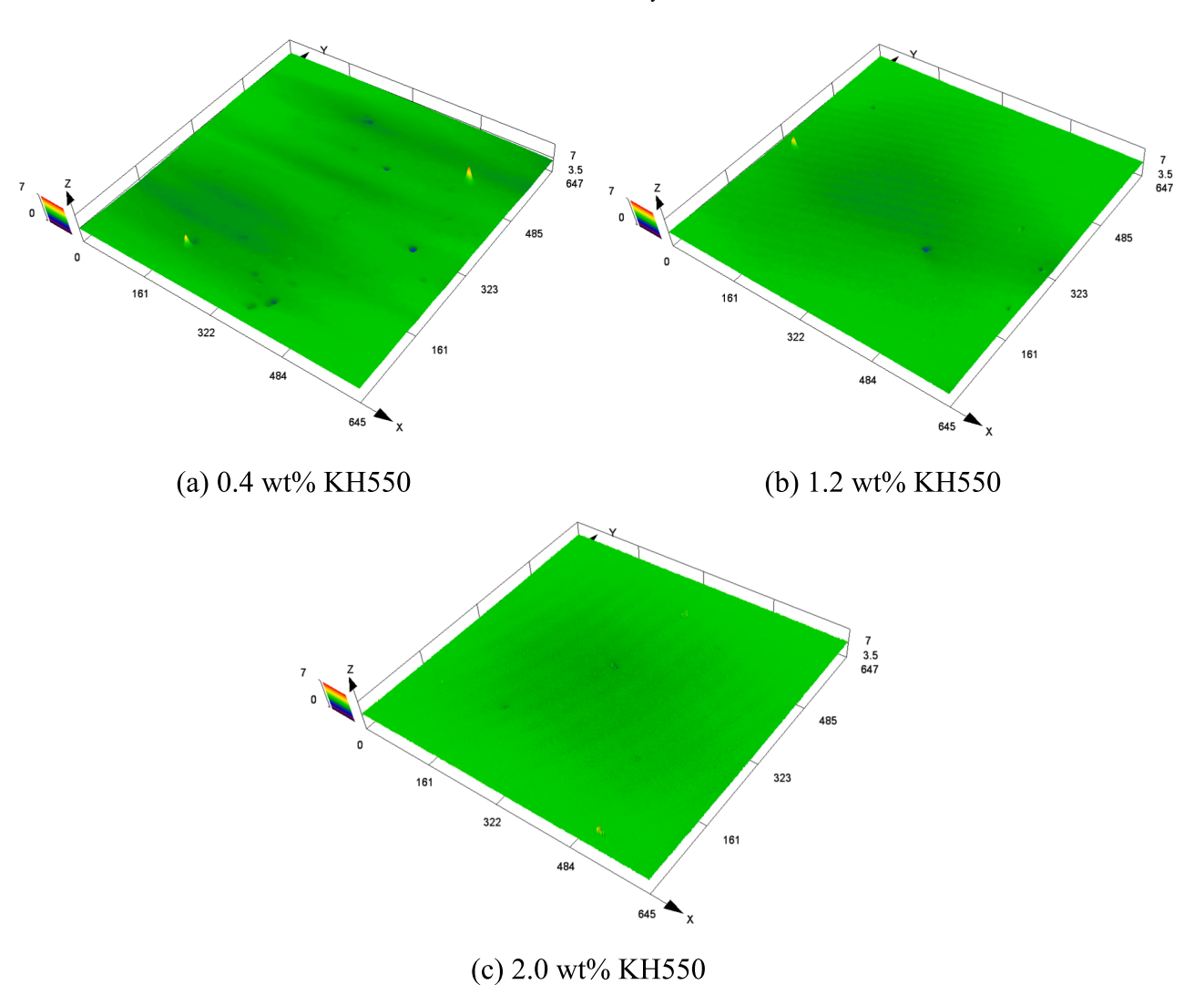
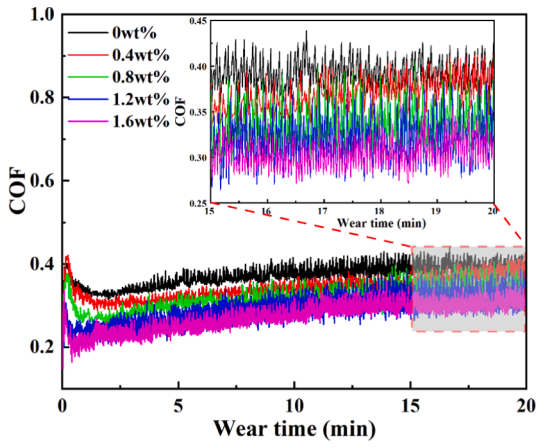
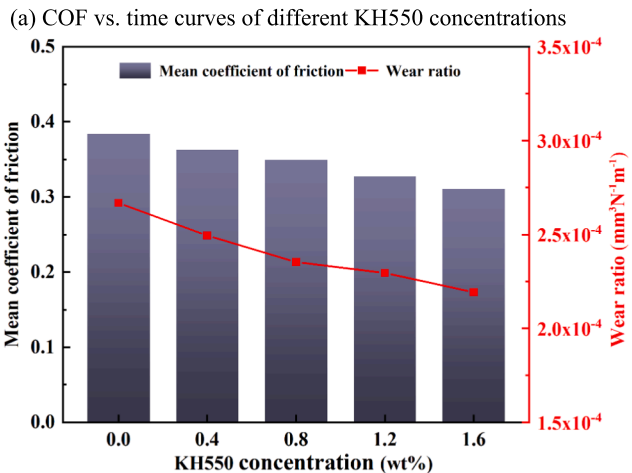


Fig. 12. Surface microstructure of K9 optical glass polished with different KH550 concentration.





(b) Mean COF and wear ratio for different KH550 concentrations

Fig. 13. Effect of KH550 concentration on COF and wear ratio.

 $\rm mm^3~N^{-1}~m^{-1}.$  The mean COF and wear ratio are lower than those without addition. KH550 adsorbs on the K9 optical glass surface and forms a lubrication film, which changes the lubrication between the grinding ball and the K9 optical glass, and reduces the damage of the grinding ball on the K9 optical glass surface during the sliding process. As a result, excellent wear reduction and wear resistance can be maintained throughout the friction and wear experiment.

#### 3.8. KH550 modification analysis of SiO<sub>2</sub> abrasive particle

To further reveal the interaction between KH550 and SiO2 abrasive particle, the effect of KH550 on the chemical bonding characteristics of the SiO<sub>2</sub> abrasive particle surface is investigated by FTIR technique as shown in Fig. 14. The telescopic vibrational peak of the O-H group is observed at a wavelength of 3430 cm<sup>-1</sup>, which is associated with the physical water absorption on the SiO2 abrasive particle surface. The peak is weakened by the addition of KH550, indicating that KH550 combines with SiO<sub>2</sub> abrasive particles and part of the O-H is replaced, thus hindering the bonding of SiO<sub>2</sub> abrasive particles with water molecules. The spectra show characteristic peaks of SiO2 abrasive particle at 1104 cm<sup>-1</sup>, 800 cm<sup>-1</sup> and 472 cm<sup>-1</sup>, which indicates the antisymmetric telescopic vibrational peak, the symmetric vibrational peak and the bending vibrational peak of the Si-O-Si bond, respectively [49]. Compared with the spectra of pure SiO<sub>2</sub> abrasive particles, the addition of KH550 resulted in new vibrational peaks, with Si-CH2 stretching vibrational peaks and bending vibrational peaks appearing at 2924 cm<sup>-1</sup>, 2848 cm<sup>-1</sup> and 1382 cm<sup>-1</sup>. The bending vibrational peak of Si-OH appeared at 1630 cm<sup>-1</sup>. The bending vibrational peak of N-H in

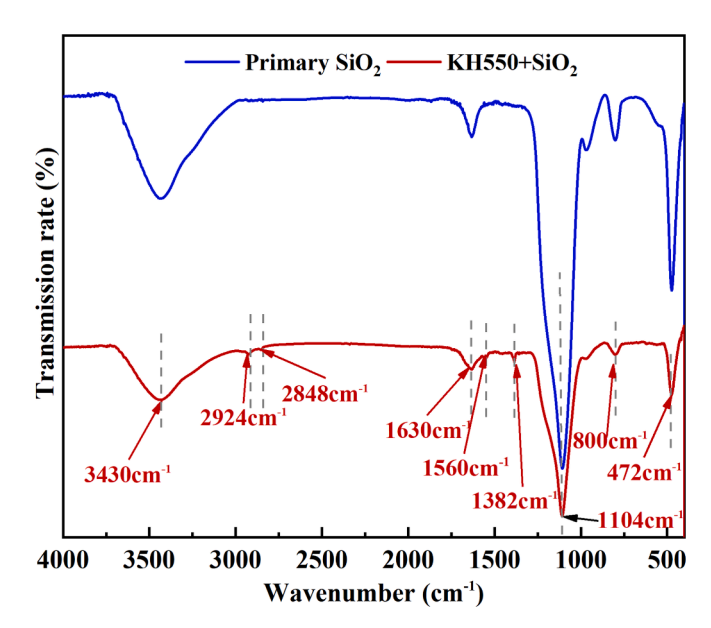


Fig. 14. FTIR plot of  ${\rm SiO_2}$  abrasive particles before and after modification by KH550.

the  $-N-H_2$  group is found at 1560 cm<sup>-1</sup> [50,51].

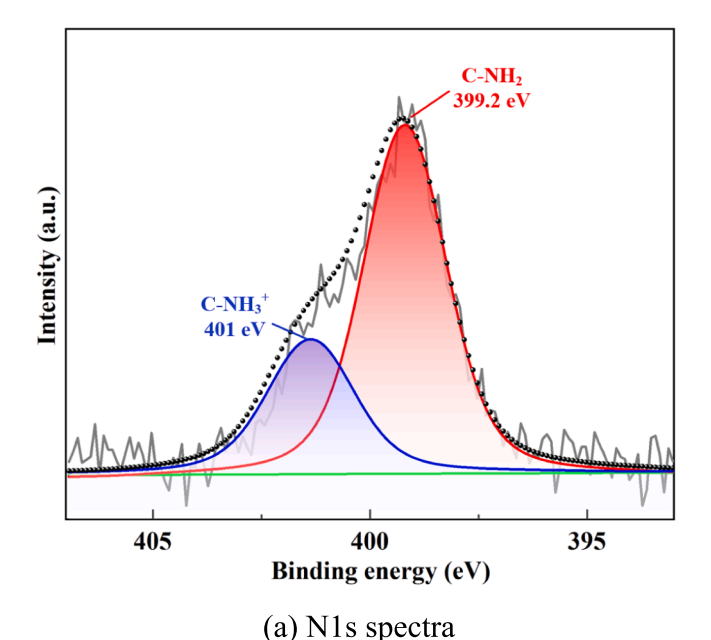
The experimental results showed that KH550 reduced the hydroxyl groups and formed new organic groups, which then modified the  ${\rm SiO_2}$  abrasive particles. It is known that the organic groups can change the stability of  ${\rm SiO_2}$  abrasive particles in the polishing slurry, increase the solubility of  ${\rm SiO_2}$  abrasive particles and reduce the agglomeration of abrasive particles according to the principle of similar solubility. Because of the strong hydrophilicity of the amino functional group (–NH<sub>2</sub>), it makes KH550 have a better dissolution in the polishing slurry, which contributes to the bonding of KH550 with the abrasive particle surface [52]. As the KH550 concentration increases, KH550 adheres to the  ${\rm SiO_2}$  abrasive particle surface, forming a "soft-shell abrasive particle" and inducing a slight increase in abrasive particle size. The analytical results are consistent with the experimental results in section 3.5.

## 3.9. Adsorption mechanism analysis of KH550 on K9 optical glass

Fig. 15 illustrates the N1s spectra and Si2p spectra of the K9 optical glass surface after immersion in solution 4 from Table 1. It can be seen from Fig. 15(a) that the immersed optical glass surface contains two characteristic peaks associated with -NH, which are the amino group (C-NH<sub>2</sub>) with the binding energy located at 399.2 eV and the protonated amine (C-NH<sub>3</sub>) with the binding energy located at 401 eV, which are induced by the combination of the C-NH<sub>2</sub> group with hydrogen (H) [53]. The peak area ratios of C-NH<sub>2</sub> and C-NH<sub>3</sub> are 71.03 % and 28.97 %, respectively. Since only KH550 contains N element in solution 4, the N1s spectra show that KH550 occurs chemical reaction with K9 optical glass and adsorbs on its surface. Three different characteristic peaks can be observed from the Si2p spectra in Fig. 15(b). There are the characteristic peaks of SiO<sub>2</sub> at 102.5 eV and Si-OH at 103.0 eV analyzed in section 3.34, but the peak area ratio is reduced to 78.73 % and 19.76 %, respectively. After the addition of KH550, the amino silane (Si-O) characteristic peak appeared at 102.2 eV, which is the characteristic peak corresponding with KH550 adsorption on optical glass, with a peak area ratio of 1.51 % [53]. This proves that KH550 is adsorbed on the K9 optical glass surface by chemical bonding.

#### 3.10. Effect of ultrasonic vibration on polishing performance

The CMP (A = 0  $\mu$ m) and UV-CMP (A = 3  $\mu$ m, 6  $\mu$ m) polishing



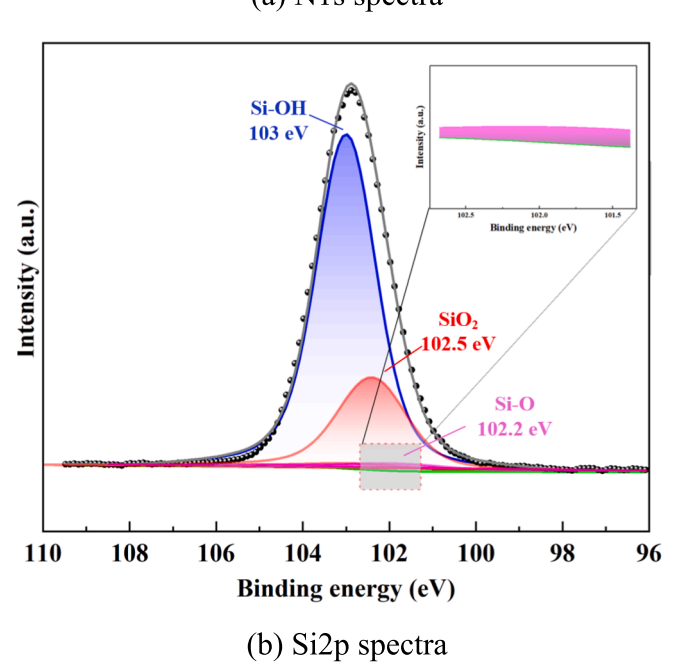


Fig. 15. XPS spectra of K9 optical glass surface.

experiments were carried out using polishing slurry containing 1.5 wt%  $K_2CO_3$ , 1.6 wt% KH550 and pH = 12. The MRR was 12.3246 µm/min,  $13.4518 \,\mu\text{m/min}$  and  $14.5298 \,\mu\text{m/min}$  at ultrasonic amplitudes of  $0 \,\mu\text{m}$ ,  $3~\mu m$  and  $6~\mu m$ , respectively, with a maximum increase of 17.89 %. The Sa value was 75.24 nm, 58.98 nm and 54.07 nm, respectively, with a maximum decrease of 28.14 %. As shown in Fig. 16(a), the workpiece surface is subjected to the scratching action of the SiO<sub>2</sub> abrasive particles to accomplish material removal in CMP. The polished surface is left with uneven scratches and large-sized pits. Fig. 16(b) and (c) show the microstructures for different axial ultrasonic amplitudes. Compared with CMP, UV-CMP utilizes ultrasonic vibration energy to provide stronger impact kinetic energy to the SiO2 abrasive particles. With the increase of ultrasonic amplitude, the high-frequency vibration enables the abrasive particles to obtain a larger motion path and higher impact velocity, accompanied by an obvious ultrasonic cavitation effect, thus significantly increasing the MRR, the original surface defects are gradually removed, and the surface quality is gradually improved.

Based on the above research results and analysis, combined with the softening mechanism of hydration reaction on the workpiece surface and the adsorption mechanism of KH550, the synergistic removal mechanism of  $\rm K_2CO_3$ , KH550 and ultrasonic vibration in UV-CMP is shown in Fig. 17.

The chemical interaction of K<sub>2</sub>CO<sub>3</sub> in an alkaline polishing slurry softens the workpiece surface, enhances the hydration reaction rate and accelerates the thickness of the hydrated layer. The Si-O-Si bond is broken and bonded with OH- to form silanol (Si-OH). The double electric layer structures of the abrasive particle and optical glass surface are compressed under the effect of K+, which enhances their electrostatic interaction and mechanical contact. KH550 modifies  ${
m SiO_2}$  abrasive particles, and its self-contained (CH<sub>2</sub>)<sub>3</sub>NH<sub>2</sub> group hinders abrasive particle agglomeration and contributes to abrasive particle dispersion. Meanwhile, KH550 adsorbs on the abrasive particles and the K9 optical glass. The impact of abrasive particles on the workpiece surface under ultrasonic vibration induces the cavitation effect and the local temperature increase in the polishing slurry, according to Chen et al [54]. It can be concluded that the large amount of energy generated by ultrasonic vibration prompts the hydrolysis of KH550 and its bonding with O-Si-O bonds formed by the hydration reaction of SiO<sub>2</sub> abrasive particles and optical glass surfaces. With the flow of polishing slurry in the contact area, the SiO2 abrasive particles detach from the bond, and the Si-O bond of the hydration layer on the optical glass surface is broken, bringing the hydration product away from the contact area to achieve the surface material removal.

#### 4. Conclusion

In this paper, a novel chemical polishing slurry with  ${\rm SiO_2}$  abrasive particle is produced by combining  ${\rm K_2CO_3}$ , KH550 and ultrasonic vibration technology for the precision polishing of K9 optical glass. The polishing characteristics and mechanism are investigated through the analysis of the chemical polishing slurry performance, the local microstructure, material removal efficiency and phase transformation. The following conclusions are obtained:

- (1) With the increase of  $K_2CO_3$  concentration, the abrasive particle size increases, the PDI value increases, and the absolute value of zeta potential decreases, thus lowering the chemical polishing slurry stability.  $K_2CO_3$  accelerates the hydration reaction rate on the K9 optical glass surface, resulting in a thicker hydrated layer, which facilitates  $SiO_2$  abrasive particle removal and improves MRR. The maximum MRR is  $13.1785 \, \mu m/min$  with a poor surface quality of  $75.32 \, nm$  at  $2.0 \, wt\% \, K_2CO_3$ .
- (2) KH550 enhances chemical polishing slurry stability and surface quality while reducing wear ratio and COF. As the KH550 concentration grows, the SiO<sub>2</sub> abrasive particle size is increased slightly, the PDI value is reduced and the absolute value of zeta potential is increased, resulting in a stabilized slurry and improved particle dispersion. The MRR is increased while the surface quality is improved. The optimal surface quality is 48.93 nm at 2.0 wt% KH550, then the MRR is 13.0382 μm/min.
- (3) The UV-CMP achieves precision processing of K9 optical glass through the combined effects of ultrasonic vibration, K<sub>2</sub>CO<sub>3</sub> and KH550. K<sub>2</sub>CO<sub>3</sub> compresses the double electric layer, enhancing electrostatic and mechanical contact. Ultrasonic vibration causes abrasive particles to impact the workpiece surface, inducing cavitation and local temperature rise, which promotes KH550 hydrolysis. Hydrolysis products bond with O-Si-O from hydration on SiO<sub>2</sub> abrasives and the glass surface. Ultrasonic vibrationinduced slurry flow removes hydration products, improving polishing performance. This process ensures uniform abrasive distribution, strong shock loading and fluid invasion, accelerating hydrated layer generation and removal.

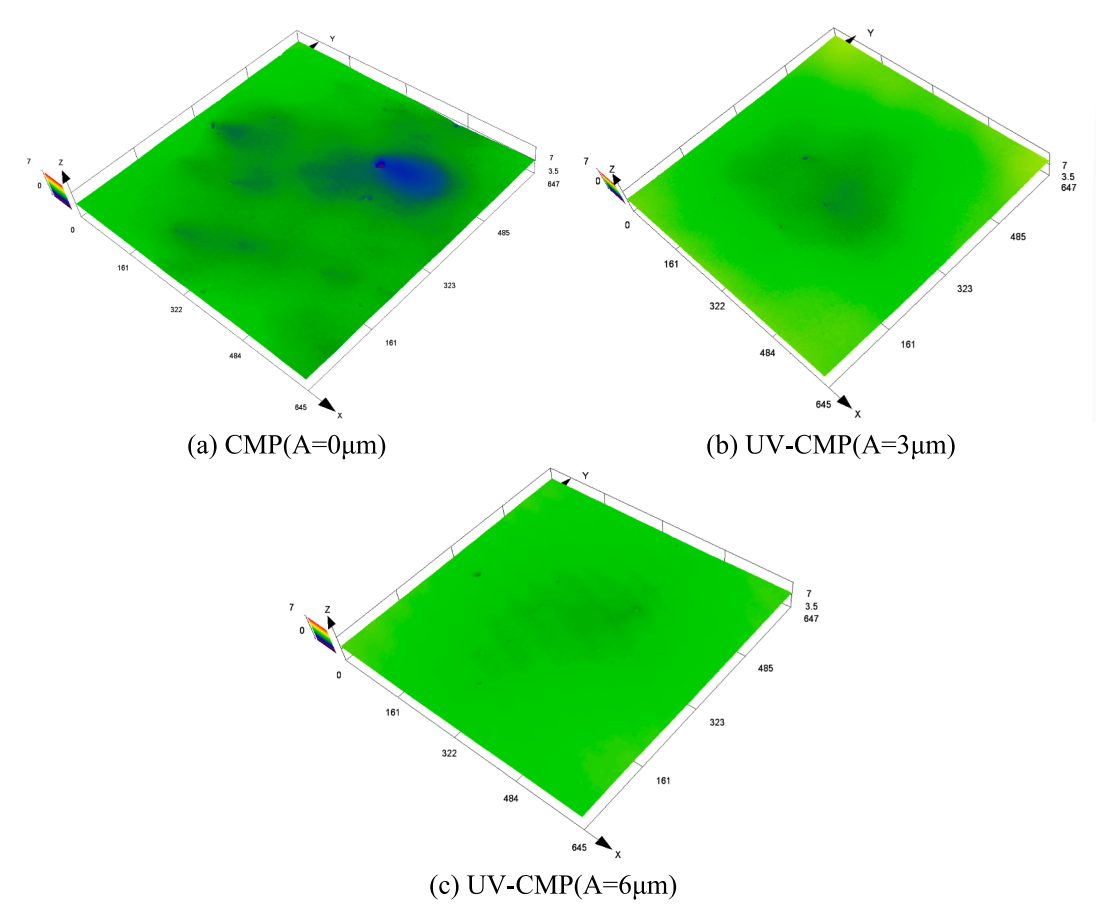


Fig. 16. Surface microstructure of K9 optical glass polished with different ultrasonic amplitude.

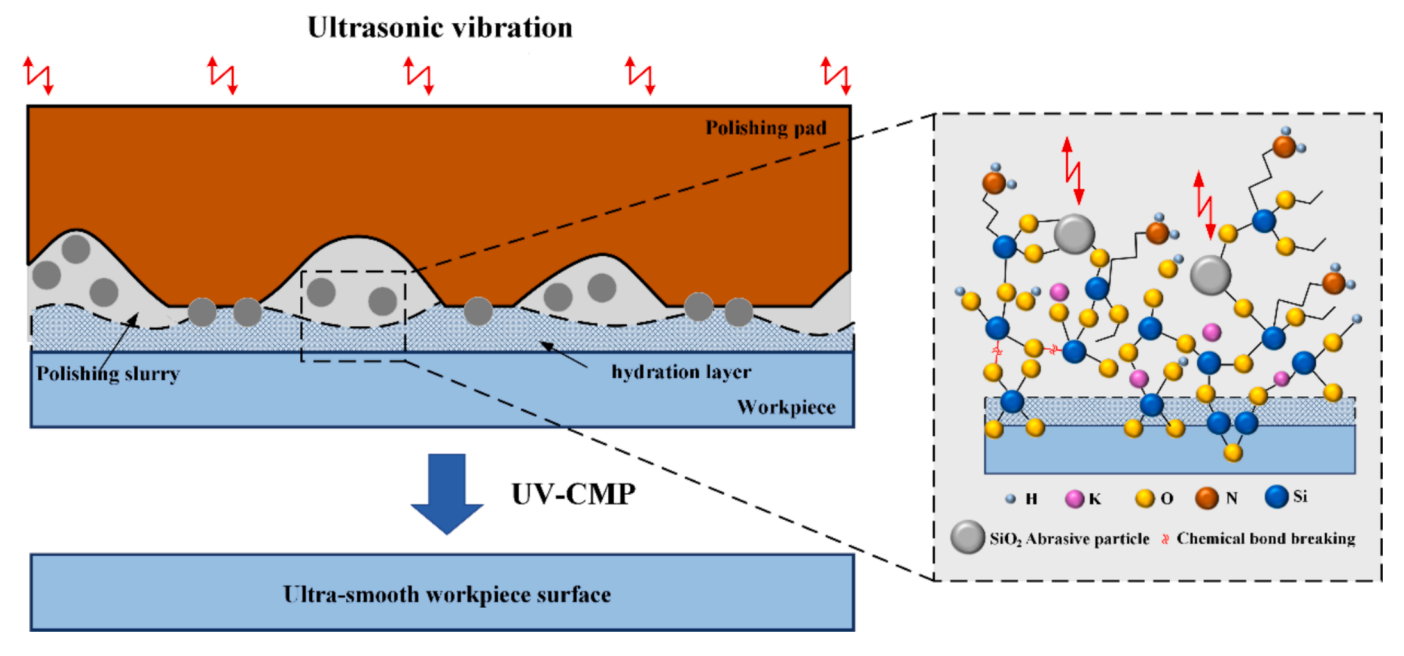


Fig. 17. Schematic diagram of the material removal mechanism of K<sub>2</sub>CO<sub>3</sub>-KH550 in UV-CMP on K9 optical glass.

The research results will further advance the development and utilization of innovative polishing slurry for K9 optical glass. In the future, the feasibility and cost-effectiveness of this advanced polishing slurry will be validated in industrial production, facilitating its integration into practical manufacturing processes to enable high-efficiency polishing of

K9 optical glass.

## CRediT authorship contribution statement

Sheng Qu: Writing - review & editing, Writing - original draft,

Validation, Software, Methodology, Formal analysis, Data curation. Zhijie Cui: Validation, Software. Xuchen Chu: Validation, Formal analysis. Xingwei Sun: Software, Funding acquisition. Zhixu Dong: Software, Funding acquisition. Heran Yang: Visualization, Formal analysis. Yin Liu: Validation, Formal analysis. Zixuan Wang: Funding acquisition. Tianbiao Yu: Supervision, Project administration. Ji Zhao: Funding acquisition.

#### Declaration of competing interest

The authors declare that they have no known competing financial interests or personal relationships that could have appeared to influence the work reported in this paper.

#### Acknowledgments

The authors would like to appreciate the financial support provided by the Liaoning Provincial Natural Science Foundation of China [Grant No. 2024-BSLH-203], the Project of Liaoning Province Applied Basic Research Program [Grant No. 2022JH2/101300214], the National Natural Science Foundation of China [Grant No. 52405460] and Liaoning Provincial Natural Science Foundation of China [Grant No. 2023-MSBA-032].

#### Data availability

Data will be made available on request.

#### References

- [1] J. Zhao, J. Huang, R. Wang, H.R. Peng, W. Hang, S. Ji, Investigation of the optimal parameters for the surface finish of K9 optical glass using a soft abrasive rotary flow polishing process, J. Manuf. Process. 49 (2020) 26–34, https://doi.org/ 10.1016/j.jmapro.2019.11.011.
- [2] M. Li, T. Yu, L. Yang, H. Li, R. Zhang, W. Wang, Parameter optimization during minimum quantity lubrication milling of TC4 alloy with graphene-dispersed vegetable-oil-based cutting fluid, J. Clean. Prod. 209 (2019) 1508–1522, https:// doi.org/10.1016/j.jclepro.2018.11.147.
- [3] C. Li, Y. Piao, F. Zhang, Y. Zhang, Y. Hu, Y. Wang, Understand anisotropy dependence of damage evolution and material removal during nanoscratch of MgF2 single crystals, Int. J. Extrem. Manuf. 5 (2023), https://doi.org/10.1088/ 2631-7990/ac9ed.
- [4] J. Zhao, J. Ge, A. Khudoley, H. Chen, Numerical and experimental investigation on the material removal profile during polishing of inner surfaces using an abrasive rotating jet, Tribol. Int. 191 (2024) 109125, https://doi.org/10.1016/j. triboint.2023.109125.
- [5] S. Qu, Z. Wang, C. Zhang, Z. Ma, T. Zhang, H. Chen, Z. Wang, T. Yu, J. Zhao, Material removal profile prediction and experimental validation for obliquely axial ultrasonic vibration-assisted polishing of K9 optical glass, Ceram. Int. 47 (2021) 33106–33119, https://doi.org/10.1016/j.ceramint.2021.08.212.
- [6] R. Pan, W. Zhao, B. Zhong, D. Chen, Z. Wang, C. Zha, J. Fan, Evaluation of removal characteristics of bonnet polishing tool using polishing forces collected online, J. Manuf. Process. 47 (2019) 393–401, https://doi.org/10.1016/j. imapro.2019.03.029.
- [7] Y. Guo, S. Yin, H. Ohmori, M. Li, F. Chen, S. Huang, A novel high efficiency magnetorheological polishing process excited by Halbach array magnetic field, Precis. Eng. 74 (2022) 175–185, https://doi.org/10.1016/j. precisioneng.2021.11.011.
- [8] D. Kang, P. Zou, H. Wu, W. Wang, J. Xu, Research on ultrasonic vibration-assisted laser polishing of the 304 stainless steel, J. Manuf. Process. 62 (2021) 403–417, https://doi.org/10.1016/j.imapro.2020.12.009.
- [9] C. Qin, Z. Hu, A. Tang, Z. Yang, S. Luo, An efficient material removal rate prediction model for cemented carbide inserts chemical mechanical polishing, Wear 452–453 (2020) 203293, https://doi.org/10.1016/j.wear.2020.203293.
- [10] W. Liu, Q. Xiong, J. Lu, X. Wang, Q. Yan, Tribological behavior of single crystal diamond based on UV photocatalytic reaction, Tribol. Int. 175 (2022) 107806, https://doi.org/10.1016/j.triboint.2022.107806.
- [11] S. Yuan, X. Guo, H. Wang, S. Gao, A Theoretical and Experimental Study on High-Efficiency and Ultra-Low Damage Machining of Diamond, J. Manuf. Sci. Eng. 145 (2023) 1–7, https://doi.org/10.1115/1.4057008.
- [12] H. Deng, K. Endo, K. Yamamura, Damage-free finishing of CVD-SiC by a combination of dry plasma etching and plasma-assisted polishing, Int. J. Mach. Tools Manuf. 115 (2017) 38–46, https://doi.org/10.1016/j. iimachtools.2016.11.002.
- [13] S. Qu, C. Zhang, Y. Liang, Z. Ma, F. Meng, Z. Wang, P. Xu, T. Yu, J. Zhao, Experimental investigation of ultrasonic-vibration polishing of K9 optical glass

- based on ultrasonic atomization, Ceram. Int. 48 (2022) 9067–9074, https://doi.org/10.1016/j.ceramint.2021.12.090.
- [14] Y. Ichida, R. Sato, Y. Morimoto, K. Kobayashi, Material removal mechanisms in non-contact ultrasonic abrasive machining, Wear 258 (2005) 107–114, https://doi. org/10.1016/j.wear.2004.05.016.
- [15] S. Qu, X. Sun, Z. Dong, Y. Liu, H. Yang, W. Zhang, Tribology International Simulation and experimental investigation of material removal profile based on ultrasonic vibration polishing of K9 optical glass, Tribol. Int. 196 (2024) 109730, https://doi.org/10.1016/j.triboint.2024.109730.
- [16] T. Zhang, C. Guan, C. Zhang, W. Xi, T. Yu, J. Zhao, Predictive modeling and experimental study of generated surface-profile for ultrasonic vibration-assisted polishing of optical glass BK7 in straight feeding process, Ceram. Int. 47 (2021) 19809–19823, https://doi.org/10.1016/j.ceramint.2021.03.320.
- [17] M.Y. Tsai, W.Z. Yang, Combined ultrasonic vibration and chemical mechanical polishing of copper substrates, Int. J. Mach. Tools Manuf. 53 (2012) 69–76, https://doi.org/10.1016/j.ijmachtools.2011.09.009.
- [18] M. Zhou, Y. Cheng, M. Zhong, W. Xu, Macro and micro-nano machining mechanism for ultrasonic vibration assisted chemical mechanical polishing of sapphire, Appl. Surf. Sci. 640 (2023) 158343, https://doi.org/10.1016/j. apsusc.2023.158343.
- [19] D. Liu, R. Yan, T. Chen, Material removal model of ultrasonic elliptical vibrationassisted chemical mechanical polishing for hard and brittle materials, Int. J. Adv. Manuf. Technol. 92 (2017) 81–99, https://doi.org/10.1007/s00170-017-0081-z.
- [20] X. Chen, Y. Liang, Z. Cui, F. Meng, C. Zhang, L. Chen, T. Yu, J. Zhao, Study on material removal mechanism in ultrasonic chemical assisted polishing of silicon carbide, J. Manuf. Process. 84 (2022) 1463–1477, https://doi.org/10.1016/j. jmapro.2022.11.014.
- [21] S. Liang, X. Jiao, X. Tan, J. Zhu, Effect of solvent film and zeta potential on interfacial interactions during optical glass polishing, Appl. Opt. 57 (2018) 5657, https://doi.org/10.1364/ao.57.005657.
- [22] S.A. Gold, V.A. Burrows, Influence of K[sup +] Ions on the Interaction of Water with Silicon Dioxide at Low Temperature Relevant to CMP, J. Electrochem. Soc. 151 (2004) G762, https://doi.org/10.1149/1.1806823.
- [23] G. Xu, Z. Zhang, F. Meng, L. Liu, D. Liu, C. Shi, X. Cui, J. Wang, W. Wen, Atomic-scale surface of fused silica induced by chemical mechanical polishing with controlled size spherical ceria abrasives, J. Manuf. Process. 85 (2023) 783–792, https://doi.org/10.1016/j.jmapro.2022.12.008.
- [24] H. Song, L.Y. Wang, W.L. Liu, Z.T. Song, Effect of cations on the chemical mechanical polishing of SiO<sub>2</sub> film, Chinese Phys. Lett. 30 (2013), https://doi.org/ 10.1088/0256-307X/30/9/098103.
- [25] W. Xie, Z. Zhang, X. Chen, S. Yu, C. Shi, H. Zhou, W. Wen, Effect of cations on the improvement of material removal rate of silicon wafer in chemical mechanical polishing, Colloids Surf. A Physicochem. Eng. Asp. 670 (2023) 131576, https://doi. org/10.1016/j.colsurfa.2023.131576.
- [26] K.-H. Bu, B.M. Moudgil, Selective Chemical Mechanical Polishing Using Surfactants, J. Electrochem. Soc. 154 (2007) H631, https://doi.org/10.1149/ 1.2734802.
- [27] J. Li, C. Zhang, P. Cheng, X. Chen, W. Wang, J. Luo, AFM Studies on Liquid Superlubricity between Silica Surfaces Achieved with Surfactant Micelles, Langmuir 32 (2016) 5593–5599, https://doi.org/10.1021/acs.langmuir.6b01237.
- [28] S. Kim, J.H. So, D.J. Lee, S.M. Yang, Adsorption behavior of anionic polyelectrolyte for chemical mechanical polishing (CMP), J. Colloid Interface Sci. 319 (2008) 48–52, https://doi.org/10.1016/j.jcis.2007.11.004.
   [29] N.K. Penta, H.P. Amanapu, B.C. Peethala, S.V. Babu, Use of anionic surfactants for
- [29] N.K. Penta, H.P. Amanapu, B.C. Peethala, S.V. Babu, Use of anionic surfactants for selective polishing of silicon dioxide over silicon nitride films using colloidal silicabased slurries, Appl. Surf. Sci. 283 (2013) 986–992, https://doi.org/10.1016/j. apsusc.2013.07.057.
- [30] L. Hao, T. Gao, W. Xu, X. Wang, S. Yang, X. Liu, Preparation of crosslinked polysiloxane/SiO 2 nanocomposite via in-situ condensation and its surface modification on cotton fabrics, Appl. Surf. Sci. 371 (2016) 281–288, https://doi. org/10.1016/j.apsusc.2016.02.204.
- [31] X. Niu, T. Wu, X. Zhao, B. Tan, Y.L. Liu, Study on CMP Mechanism and Technology of Sapphire Substrate for Photo-conducting Device, ECS Trans. 18 (2009) 435–440, https://doi.org/10.1149/1.3096482.
- [32] C.Y. Yu, Y.F. Gao, B. Han, M. Ehrhardt, P. Lorenz, L.F. Xu, R.H. Zhu, Picosecond laser induced periodic surface structures on K9 glass, Surf. Interfaces 23 (2021), https://doi.org/10.1016/j.surfin.2021.101026.
- [33] W. Xie, Z. Zhang, S. Yu, L. Li, X. Cui, Q. Gu, et al., High efficiency chemical mechanical polishing for silicon wafers using a developed slurry, Surf. Interfaces 38 (2023), https://doi.org/10.1016/j.surfin.2023.102833.
- [34] L. Wang, S. Wang, Quantitative analysis of self-healing properties and microstructure of Ti-5Al-5Mo-5V-1Cr-1Fe alloy by quasi-in-situ XPS, J. Alloys Compd. 1012 (2025) 178509, https://doi.org/10.1016/j.jallcom.2025.178509.
- [35] W. Choi, U. Mahajan, S.-M. Lee, J. Abiade, R.K. Singh, Effect of Slurry Ionic Salts at Dielectric Silica CMP, J. Electrochem. Soc. 151 (2004) G185, https://doi.org/ 10.1140/1.1644600
- [36] X. Zhao, X. Niu, D. Yin, J. Wang, K. Zhang, Research on R-Plane Sapphire Substrate CMP Removal Rate Based on a New-Type Alkaline Slurry, ECS J. Solid State Sci. Technol. 7 (2018) P135–P141, https://doi.org/10.1149/2.0241803jss.
- [37] L. Ye, Z. Baoguo, Z. Li Haoran, W. Pengfei, W. Ye, X. Mengchen, Effect of alkali metal ion on chemical mechanical polishing of LiTaO<sub>3</sub>, ECS J. Solid State Sci. Technol. 11 (2022) 034003, https://doi.org/10.1149/2162-8777/ac5474.
- [38] I.U. Vakarelski, N. Teramoto, C.E. McNamee, J.O. Marston, K. Higashitani, Ionic enhancement of silica surface nanowear in electrolyte solutions, Langmuir 28 (2012) 16072–16079, https://doi.org/10.1021/la303223q.

- [39] N. Tufenkji, M. Elimelech, Deviation from the classical colloid filtration theory in the presence of repulsive DLVO interactions, Langmuir 20 (2004) 10818–10828, https://doi.org/10.1021/la0486638.
- [40] J.F. Carstens, J. Bachmann, I. Neuweiler, A new approach to determine the relative importance of DLVO and non-DLVO colloid retention mechanisms in porous media, Colloids Surf. A Physicochem. Eng. Asp. 560 (2019) 330–335, https://doi.org/ 10.1016/j.colsurfa.2018.10.013.
- [41] R. Huang, C. Ma, Q. He, J. Ma, C. Liu, Z. Wu, X. Huangfu, Transport behaviors of colloidal manganese dioxide in aqueous media: effects of ionic specificity of monovalent cations, J. Phys. Chem. C. 124 (2020) 16371–16380, https://doi.org/ 10.1021/acs.jpcc.0c03022.
- [42] C. Park, H. Kim, H. Cho, T. Lee, D. Kim, S. Lee, H. Jeong, Effect of relative surface charge of colloidal silica and sapphire on removal rate in chemical mechanical polishing, Int. J. Precis. Eng. Manuf. - Green Technol. 6 (2019) 339–347, https:// doi.org/10.1007/s40684-019-00020-9.
- [43] J. Zhou, X. Niu, Z. Wang, Y. Cui, J. Wang, C. Yang, Z. Huo, R. Wang, Roles and mechanism analysis of chitosan as a green additive in low-tech node copper film chemical mechanical polishing, Colloids Surf. A Physicochem. Eng. Asp. 586 (2020) 124293, https://doi.org/10.1016/j.colsurfa.2019.124293.
- [44] C. Yao, X. Niu, C. Wang, Y. Liu, Z. Jiang, Y. Wang, S. Tian, Study on the Weakly Alkaline Slurry of Copper Chemical Mechanical Planarization for GLSI, ECS J. Solid State Sci. Technol. 6 (2017) P499–P506, https://doi.org/10.1149/2.0071708jss.
- [45] S.R. Darmakkolla, H. Tran, A. Gupta, S.B. Rananavare, A method to derivatize surface silanol groups to Si-alkyl groups in carbon-doped silicon oxides, RSC Adv. 6 (2016) 93219–93230, https://doi.org/10.1039/c6ra20355h.
- [46] Y. Kong, P. Wang, S. Liu, Z. Gao, M. Rao, Effect of microwave curing on the hydration properties of cement-based material containing glass powder, Constr BuildMater 158 (2018) 563–573, https://doi.org/10.1016/j. conbuildmat.2017.10.058.

- [47] T.S. Mahadevan, J. Du, Hydration and reaction mechanisms on sodium silicate glass surfaces from molecular dynamics simulations with reactive force fields, J. Am. Ceram. Soc. 103 (2020) 3676–3690, https://doi.org/10.1111/jace.17059.
- [48] C. Wei, Y. Tian, O.F. Ogunbiyi, J. Han, X. Fan, Z. Gu, Effects of abrasive grain size of flexible body-armor-like abrasive tool (BAAT) on high-shear and low-pressure grinding for zirconia ceramics, J. Manuf. Process. 120 (2024) 827–836, https:// doi.org/10.1016/j.jmapro.2024.05.012.
- [49] G.S. Pan, Z.H. Gu, Y. Zhou, T. Li, H. Gong, Y. Liu, Preparation of silane modified SiO<sub>2</sub> abrasive particles and their Chemical Mechanical Polishing (CMP) performances, Wear 273 (2011) 100–104, https://doi.org/10.1016/j. wear.2011.05.044.
- [50] M. Najafi, Y. Yousefi, A.A. Rafati, Synthesis, characterization and adsorption studies of several heavy metal ions on amino-functionalized silica nano hollow sphere and silica gel, Sep. Purif. Technol. 85 (2012) 193–205, https://doi.org/ 10.1016/j.seppur.2011.10.011.
- [51] A. Hou, H. Chen, Preparation and characterization of silk/silica hybrid biomaterials by sol-gel crosslinking process, Mater. Sci. Eng. B. 167 (2010) 124–128, https://doi.org/10.1016/j.mseb.2010.01.065.
- [52] J. Xu, C. Wang, S. Zhou, R. Zhang, Y. Tian, Low-temperature direct bonding of Si and quartz glass using the APTES modification, Ceram. Int. 45 (2019) 16670–16675, https://doi.org/10.1016/j.ceramint.2019.05.098.
- [53] G. Jakša, B. Štefane, J. Kovač, XPS and AFM characterization of aminosilanes with different numbers of bonding sites on a silicon wafer, Surf. Interface Anal. 45 (2013) 1709–1713, https://doi.org/10.1002/sia.5311.
- [54] X. Chen, C. Zhang, F. Meng, T. Yu, J. Zhao, Polishing mechanism analysis of silicon carbide ceramics combined ultrasonic vibration and hydroxyl, Tribol. Int. 179 (2023) 108187, https://doi.org/10.1016/j.triboint.2022.108187.